

Eco-friendly and cost-effective superabsorbent sodium polyacrylate composites for environmental remediation

Yang Yu¹ · Rengui Peng¹ · Cheng Yang² · Youhong Tang¹

Received: 10 March 2015 / Accepted: 23 May 2015 / Published online: 3 June 2015
© Springer Science+Business Media New York 2015

Abstract In this research, we synthesized superabsorbent polymers (SAPs) based on poly(acrylic acid) with super adsorption properties through a novel one-step cost-effective method. The SAPs' adsorption for removal of heavy metal ions [e.g., Cu(II)] from aqueous solutions was systematically studied. The effects of pH (2.0–5.0), sodium hydroxide and water composition, contact time (0–48 h), and initial Cu(II) ion concentrations (1–500 mg dm⁻³) on the adsorption of Cu(II) ions were studied using atomic absorption spectroscopy. The adsorption behavior was fitted to a Langmuir isotherm and shown to follow a pseudo-second-order reaction model. The maximum adsorption capacities of Cu(II) ions were shown to be 243.91 mg g⁻¹ for sodium polyacrylate (PAANa), which is among the highest adsorption capacities reported in the literature. The superior adsorption capacity of Cu(II) ions is attributed to the chelating ability of functional groups (e.g., -COO⁻) in the PAANa matrix. The recyclability of the PAANa material showed that over 98.92 % of the adsorbed copper could be recovered in a mild concentration (0.01 M) of nitric acid. Results of three consecutive adsorption–desorption cycles showed that the composites had high adsorption and desorption efficiency, implying that PAANa samples can be recycled and reused as an effective adsorbent for Cu(II) recovery.

Introduction

Heavy metals are recognized as one of the most harmful pollutants in the environment, due to their detrimental effects on aquatic environments and human beings, such as high toxicity, bioaccumulation, and non-degradability [1–3]. Common sources of heavy metal pollution are mainly mining and industrial activities such as petroleum refining, paints and pigments, pesticide production, chemical manufacturing, mining and smelting activities, and electroplating [1, 4]. Common methods for removal of heavy metal ions from wastewater include coagulation, precipitation, ion exchange, filtration, adsorption, electrodeposition, and flotation [3, 5–8]. Among these, adsorption as a conventional method is considered to be the simplest, most reliable, efficient, and cost-effective method. Activated carbon is one of the most widely used materials for removal of heavy metal ions from effluents, but it requires high energy and capital cost to produce and is very difficult to regenerate [9]. Therefore, increased research has focused on developing cost-effective and environmentally friendly materials for the removal of heavy metal ions from wastewater.

Superabsorbent polymers (SAPs) are three-dimensional (3D), cross-linked hydrophilic networks of polymer chains, which have superior ability to absorb and retain ultra-high amounts (1000–100,000 %) of water in comparison to their own mass [10–12]. They can absorb solutions quickly by swelling porous structure networks to reduce mass-transfer resistance, and different functional groups (e.g., hydroxy, carboxylic acid, amine, amidoxime, and sulfonic acid groups) are present on the polymer chains that enable coordination and chelation with the metal ions [13, 14]. Due to their low-cost, non-toxicity, and biocompatibility, SAPs with different natural and synthesized fillers have been

✉ Youhong Tang
youhong.tang@flinders.edu.au

¹ Centre for NanoScale Science & Technology and Centre for Maritime Engineering, Control and Imaging, School of Computer Science, Engineering and Mathematics, Flinders University, Bedford Park, SA 5042, Australia

² Division of Energy & Environment, Graduate School of Shenzhen, Tsinghua University, Shenzhen 518055, China

widely used in water purification and applications for the recovery of metal ions [13, 15–17]. Zheng et al. incorporated starch and humic substances into polymer hydrogels, and a series of starch-g-poly(acrylic acid)/sodium humate (St-g-PAA/SH) hydrogels were synthesized for Cu(II) adsorption from the aqueous solution [18]. Wu and Li prepared a poly(hydroxyethyl methacrylate/maleamic acid) hydrogel through ^{60}Co - γ induced copolymerization and it was used for multi-metal ions [e.g., Pb(II), Cd(II), Ni(II), and Cu(II)] removal [19]. Wang et al. developed chitosan-g-poly(acrylic acid)/attapulgite (CTS-g-PAA/APT) composites to recover Cu(II) from aqueous solution, which displayed high adsorption and desorption efficiency [16]. All these methods, however, require costly chemicals, extended preparation time, special conditions (e.g., inert gas protection), and multi-step synthesis processes.

In the present work, a novel one-step, cost-effective, and environmentally friendly method was used for the synthesis of poly(acrylic acid) (PAA)-based SAPs, which requires a mild reaction condition without generating contaminated effluents. Copper was chosen as an example of heavy metal ions, and we systematically investigated the adsorption behavior of Cu(II) ions onto the PAA and sodium polyacrylate (PAANa) samples. Batch experiments were conducted to investigate the adsorption affinity, kinetics, and equilibrium loading capacity of both PAA and PAANa samples toward Cu(II) ions in aqueous solution. The impacts of NaOH concentration, surface functionality, initial metal ion concentration, and pH were also examined. Several consecutive adsorption–desorption cycles were used for the desorption of adsorbed Cu(II) ions from the adsorbents and for regeneration and reuse of the PAANa composite.

Experimental sections

Materials

Acrylic acid, ammonium persulfate (APS), and N,N' -Methylenebis(acrylamide) (MBA) were purchased from Sigma-Aldrich Australia. Sodium hydroxide, nitric acid, and potassium hydroxide were supplied from Chem Supply (Australia). All aqueous solutions were prepared using Milli-Q water (18.2 M Ω cm at 25 °C).

Synthesis of PAA and PAANa composite

Systematic diagrams of one-step synthesis of PAA and PAANa samples are shown in Scheme 1. Briefly, 3.7 g acrylic acid was dispersed in 3.5 cm³ Milli-Q water at ~ 5 °C. A standard 0.45 g cm⁻³ NaOH solution was prepared by dissolving 1.63 g sodium hydroxide powder in

3.62 g Milli-Q water followed by cooling in an ice-water bath for 10 min. Another NaOH solution with different concentrations was made by varying the mass of NaOH powder used, and 0–0.68 g cm⁻³ NaOH solution was prepared. Then, NaOH solution was added into the acrylic acid solution dropwisely with magnetic stirring at ~ 5 °C for 20 min. 0.025 g MBA and 0.08 g APS powder were added into the mixture with vigorous shaking by an IKA Vortex 3 shaker to ensure homogeneity. The mixture was then poured into a Petri dish (95 mm in diameter) and placed in an oven for 30 min with the temperature increased from 60 to 80 °C at a rate of 1 °C min⁻¹. The synthesized PAA or PAANa polymer samples were peeled off from the Petri dish and dried by vacuum desiccation at 50 °C for 1 day.

Spectroscopic analysis

Fourier transform infrared (FTIR) spectroscopy was used for functional group analysis of the different PAA samples. A FTIR PerkinElmer Spectrum 400 spectrometer equipped with an attenuated total reflectance (ATR, top-plate type) accessory was used for the FTIR investigation. Each sample (~ 0.1 g, dry) was mounted onto crystal at the center of the ATR plate, and air was used as a background reference before each scan. FTIR spectra were then recorded using 64 scans from 4000 to 550 cm⁻¹ with a resolution of 4 cm⁻¹ in absorbance mode with background subtraction.

Water absorption capacity

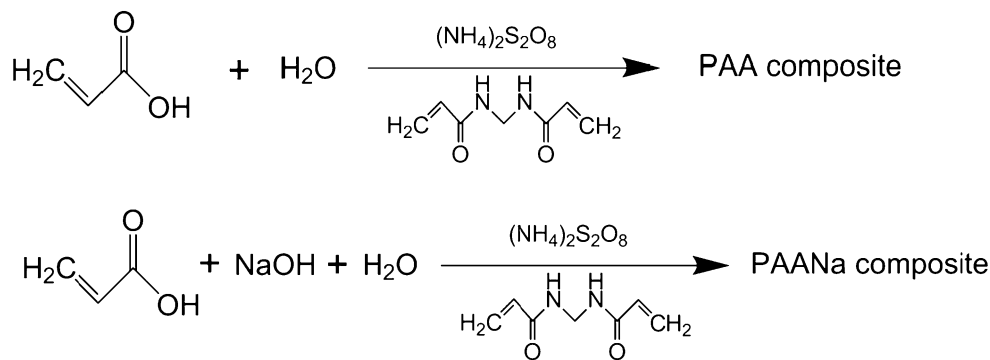
The water absorption capacity (WAC) of different PAA and PAANa samples was investigated by immersing the dry PAA/PAANa samples into excess Milli-Q water until swelling equilibrium was reached (24 h). The swollen PAA/PAANa samples were then filtered on filter paper to remove non-absorbed water on the sample surface. The WAC is calculated using Eq. 1 [20]:

$$\text{WAC} = \frac{M - M_0}{M_0}, \quad (1)$$

where M_0 and M are the PAA/PAANa sample weights before and after water absorption, respectively.

Adsorption experiments

The adsorption behavior of the PAA and PAANa sample adsorbents was investigated by varying the initial Cu(II) ion concentration from 1 to 500 mg dm⁻³. Standard solutions of Cu(II) (1–500 mg dm⁻³) were prepared by dilution of a 1000 mg dm⁻³ CuSO₄·5H₂O stock solution with Milli-Q water. The dry adsorbents (0.01 g) were dispersed

Scheme 1 Schematic diagrams of one-step synthesis of PAA and PAANa samples

in aqueous Cu(II) ion solutions (40 cm^3) with certain concentrations and the suspension was shaken by an orbital shaker (Labec, Australia) at 160 rpm for 24 h to ensure equilibrium. The suspensions were then filtered through a $0.45 \mu\text{m}$ membrane filter (Millipore, Millex-HN, Nylon, USA) and the filtrate was diluted to $<10 \text{ mg dm}^{-3}$ by Milli-Q water. The concentration of Cu(II) solution was analyzed using a flame atomic absorption spectrophotometer (FAAS) (GBC933 plus, US) with a hollow cathode lamp (photon lamps) at a wavelength of 327.4 nm and air-acetylene flame. A calibration curve was performed first, for calculation of the Cu(II) ion concentration. The effects of pH (2.0–5.0), contact time (0–48 h), and initial Cu(II) ion concentration ($1\text{--}500 \text{ mg dm}^{-3}$) on the adsorption kinetics and isotherms of the PAANa samples were investigated with at least three replicates of each experiment being performed. Hydrochloric acid (0.01 M) and potassium hydroxide (0.01 M) were used to adjust the pH of each suspension.

The Cu(II) adsorption capacity q (mg g^{-1}) and adsorption efficiency are calculated from Eqs. 2 and 3, respectively [21]:

$$q = \frac{(C_0 - C)V}{W} \quad (2)$$

$$\text{Adsorption efficiency} = \frac{(C_0 - C)}{C_0} \times 100\%, \quad (3)$$

where C_0 and C are the initial and equilibrium concentration of Cu(II) (mg dm^{-3}), respectively; V is the volume of the solution (dm^3); and W is the dry mass of the adsorbent (g).

Desorption and regeneration studies

The Cu(II)-loaded PAANa samples were recovered from the adsorption experiments by filtration washing three times with Milli-Q water, followed by vacuum desiccation at $50 \text{ }^\circ\text{C}$ for 1 day. The recovery of Cu(II) ions and the regeneration of the PAANa composite were studied using 40 cm^3 0.01 M nitric acid solution at room temperature.

Nitric acid solution was mixed with Cu(II)-loaded PAANa samples ($\sim 0.01 \text{ g}$), and the suspension was shaken at 160 rpm for 24 h for equilibration. The amount of Cu(II) recovered was determined by FAAS (GBC933 plus). Then the regenerated PAANa samples were separated from the solution by filtration and washed three times with Milli-Q water, followed by a regeneration process with 50 cm^3 Milli-Q water or $3.5 \times 10^{-4} \text{ M}$ NaOH solution which was shaken at 160 rpm for 24 h. After that, the regenerated PAANa samples were dried under vacuum desiccation at $50 \text{ }^\circ\text{C}$ for 24 h for reuse.

Results and discussion

Characterization of PAA and PAANa samples

During the polymerization process of PAA, the initiator APS is decomposed under heating and generates sulfate anion-radicals which have a strong propensity to attract hydrogen from $-\text{OH}$ groups and to form active macroradicals [22]. These macroradicals can trigger the vinyl groups of acrylic acid (AA) for chain propagation and initiate polymerization [22]. Meanwhile, the crosslinking agent MBA participates in the crosslinking reaction, enabling the formation of a polymeric cross-linked network of PAA [22]. With the neutralization of NaOH during the polymerization process, H^+ from the $-\text{COOH}$ groups in PAA chains is partially replaced by Na^+ , causing the PAA matrix to become an anionic polyelectrolyte PAANa with negatively charged $-\text{COO}^-$ in the main chain.

Figure 1a shows the FTIR spectra of the PAA and PAANa composites prepared by NaOH solution with different concentrations ($0\text{--}0.68 \text{ g cm}^{-3}$) and the PAANa sample after Cu(II) ion adsorption, respectively. For the PAA sample, no OH solution was added during the polymerization process (curve i, Fig. 1a); $-\text{C}=\text{O}$ asymmetric stretching vibrations of $-\text{COOH}$ groups were observed at 1695 cm^{-1} , and COO^- symmetric stretching vibrations of $-\text{COO}^-$ groups were observed at 1404 cm^{-1} [16, 22–25].

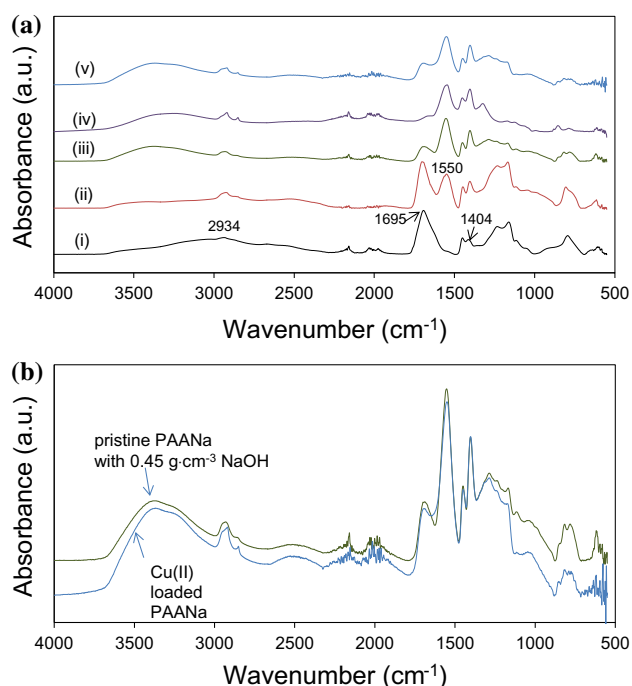


Fig. 1 **a** FTIR spectra of PAA or PAANa composites prepared with (i) 0 g cm^{-3} , (ii) 0.23 g cm^{-3} , (iii) 0.45 g cm^{-3} , and (iv) 0.68 g cm^{-3} NaOH solution, (v) PAANa sample prepared by 0.45 g cm^{-3} NaOH solution after Cu(II) adsorption. **b** Comparison of FTIR spectra of (iii) and (v)

The broad peak at 3396 cm^{-1} is attributed to the O–H stretching of water molecules in the PAA matrix [26]. The vibrations at 2934, 2859, and 1450 cm^{-1} are associated with the asymmetric and symmetric stretching of $-\text{CH}_2-$ and C–H in-plane bending, indicating the existence of a PAA main chain [23, 27]. After the increase in NaOH concentration (0.23 – 0.68 g cm^{-3}) during the polymerization process, an additional band was observed at 1500 cm^{-1} , which is attributed to $-\text{C}=\text{O}$ asymmetric stretching vibrations of $-\text{COO}^-$ groups [22]. The intensity of $-\text{C}=\text{O}$ (from the $-\text{COO}^-$ group) at 1550 cm^{-1} increased with the increase of NaOH concentration while that of $-\text{C}=\text{O}$ (from $-\text{COOH}$ groups) decreased significantly, indicating change in the molecular structure of the PAA chains. With the neutralization of NaOH, $-\text{COOH}$ groups were gradually converted into $-\text{COO}^- \text{Na}^+$ until most of the H^+ ions of the $-\text{COOH}$ groups were replaced by Na^+ and the band of $-\text{C}=\text{O}$ (from $-\text{COOH}$) at 1695 cm^{-1} disappeared (curve iv, Fig. 1a). These changes may influence the PAANa adsorption capacity of Cu(II) ions in aqueous solution compared with that of the PAA sample.

To further investigate the mechanism of Cu(II) adsorption onto the PAANa sample, a comparison of the FTIR spectra of the PAANa sample before and after Cu(II) adsorption are shown in Fig. 1b. The strong absorption band at 1550 cm^{-1} corresponding to the $-\text{C}=\text{O}$ asymmetric

stretching vibrations of $-\text{COO}^-$ groups is weakened and shifts to a lower wavenumber (1548 cm^{-1}), while the absorption band at 1695 cm^{-1} corresponding to the $\text{C}=\text{O}$ asymmetric stretching vibrations of the $-\text{COOH}$ groups is also clearly weakened. The lower intensity in the vibration of $\text{C}=\text{O}$ indicates the reorganization of the $-\text{COOH}$ molecules with Cu(II) ions, which is in agreement with the results in literature [28]. These changes in the FTIR spectra of the PAANa composites before and after Cu(II) adsorption indicate that the $-\text{COO}^-$ and $-\text{COOH}$ groups in the PAANa matrix, which have a strong propensity to chelate Cu(II) ions, were involved in the ion exchange or complexation interaction during the adsorption process of the metal ions from the aqueous solution [16, 18, 22, 29].

Adsorption studies of Cu(II) ions

The WACs of PAA and PAANa prepared with different NaOH solutions are shown in Fig. 2. Without the neutralization of NaOH, the $-\text{COOH}$ groups are protonated in the PAA matrix and the WAC of PAA (7.93 g g^{-1}) is much lower than that of the PAANa samples (48.49 – 97.93 g g^{-1}), due to the lack of anion–anion repulsive forces among the $-\text{COO}^-$ groups [30, 31]. With NaOH added during the polymerization process, $-\text{COOH}$ groups in the PAA chains were partially converted to $-\text{COO}^-$, causing the PAANa matrix to become an anionic polyelectrolyte and the WAC to increase [24]. However, the WAC reduce when a high percentage of $-\text{COOH}$ is neutralized by NaOH, which is due to a ‘charge screening effect’ of excess cations (such as Na^+ ions) in the swelling polymer which shield the $-\text{COO}^-$

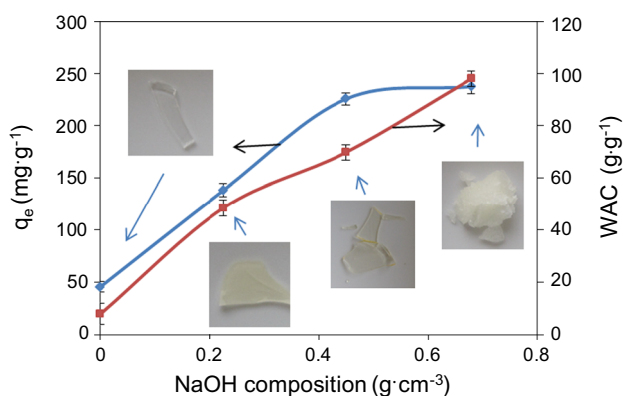


Fig. 2 Effect of NaOH composition on Cu(II) ion adsorption (left) and water absorption capacity (right) by PAA prepared with 0 g cm^{-3} NaOH solution or different PAANa composites prepared with 0.23 – 0.68 g cm^{-3} NaOH solution. (Cu(II) adsorption parameters: $\text{pH} = 5$, contact time 24 h.) The inset photo images show the morphologies of the PAA (prepared with 0 g cm^{-3} NaOH solution) or PAANa composites prepared with 0.23 – 0.68 g cm^{-3} NaOH solution

anions and decrease the anion–anion repulsion (screening/shielding effect) [30].

The effects of different NaOH compositions on Cu(II) ion adsorption by PAA or different PAANA composites are shown in Fig. 2, where the Cu(II) adsorption capacity increases as the degree of neutralization by NaOH increases. The PAA sample has the lowest Cu(II) adsorption capacity (q_e , 45.86 mg g^{-1}) whereas that of the PAANA sample prepared by 0.45 g cm^{-3} NaOH solution reaches 225.45 mg g^{-1} . Further increasing the NaOH concentration only slightly increases the q_e (237.24 mg g^{-1}), but the morphology of the sample changes from smooth transparent polymer sheets to a granular wobbly weak network (inset photo images in Fig. 2) which disintegrates into small pieces after swelling. From the FTIR result (Fig. 1a), the ratio of COO^-/COOH increases with NaOH concentration and the negatively charged COO^- groups have stronger electrostatic interaction with Cu(II) ions compared to the neutral COOH groups. For the PAA sample at $\text{pH} = 5$, although most $-\text{COOH}$ groups may ionize to $-\text{COO}^-$, the released H^+ groups still compete with Cu(II) ions during the adsorption process onto the PAA matrix. Another explanation is that the WAC increases significantly with NaOH concentration (Fig. 2). The adsorbent with a higher WAC tends to absorb water and metal ions into its matrix more easily and effectively, increasing the possibility for ion exchange and complexation of the entering Cu(II) ions with the functional groups within the adsorbent.

Since the PAANA sample prepared by 0.45 g cm^{-3} NaOH solution had a relatively high Cu(II) adsorption capacity and retained the PAA polymer structure after water absorption, it was selected for further Cu(II) adsorption and recovery experiments. The pH influences the Cu(II) ion speciation in solution and the interfacial chemistry of the adsorbents. At higher pH (>5), copper ions form $\text{Cu}(\text{OH})_2$ colloids which can precipitate from the solution and influence the accuracy of adsorption experiments [32]. Therefore, the pH range from 2 to 5 was selected for the Cu(II) ion adsorption studies. The adsorption capacity of PAANA samples (prepared by 0.45 g cm^{-3} NaOH solution) was investigated for the effectiveness of adsorption of Cu(II) ions from aqueous solution between $\text{pH} = 2$ and 5 (Fig. 3). The PAANA sample showed a maximum adsorption capacity of 232.59 mg g^{-1} at $\text{pH} = 5$, where strong electrostatic interactions existed between the positively charged Cu(II) ions and the negatively charged COO^- in the PAANA matrix, which had a strong complexation or coordination tendency with Cu(II) ions in aqueous solution (Fig. 3) [16, 18, 22, 29]. Moreover, the $-\text{COOH}$ groups were deprotonated to form COO^- when the pK_a value of PAA was around 4.30 [33]. At lower pH, Cu(II) adsorption was

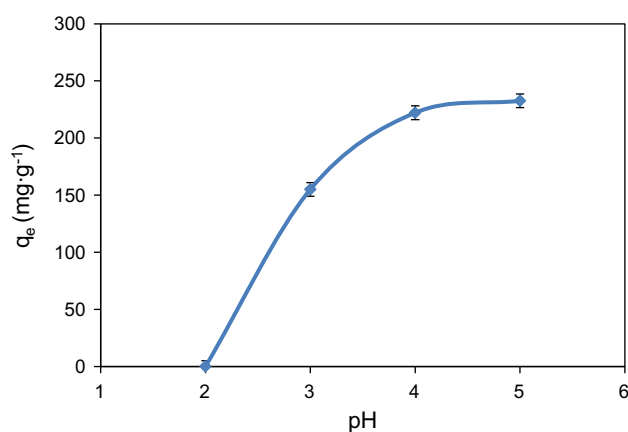


Fig. 3 Effect of pH on the adsorption of Cu(II) ions by PAA sample (prepared by 0.45 g cm^{-3} NaOH solution). Initial concentration of Cu(II) was 100 mg dm^{-3} (contact time: 24 h)

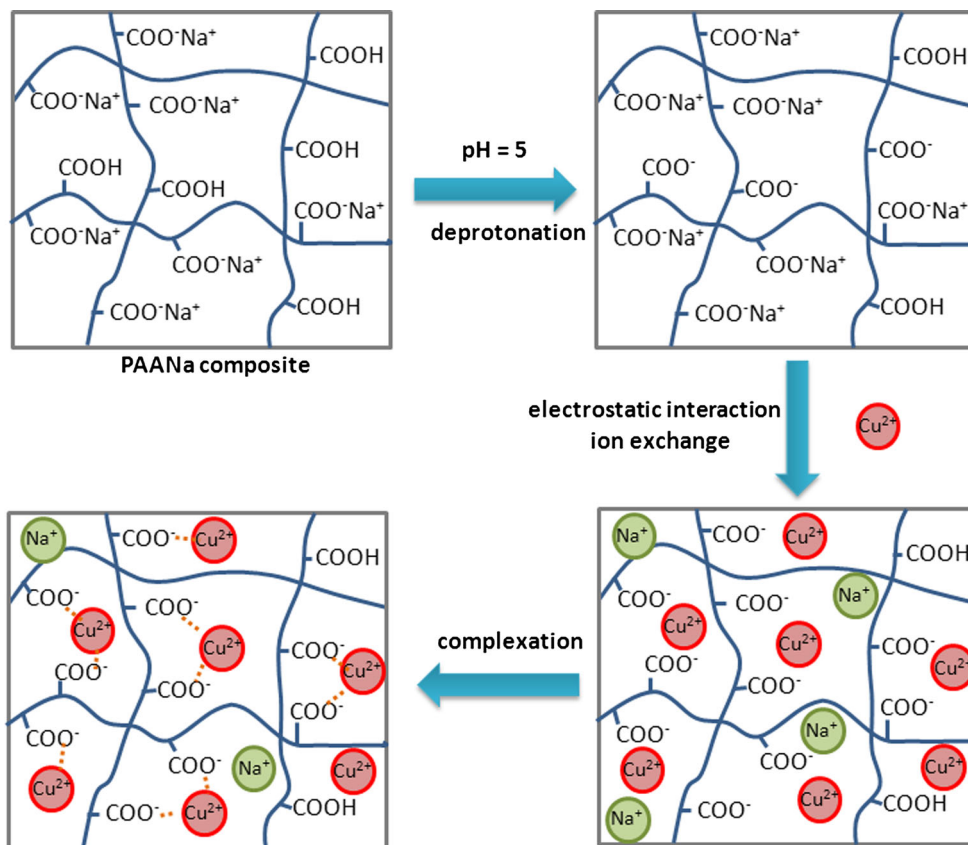
suppressed significantly due to the decrease of negative electrostatic charge through the protonation of COO^- as well as the competition between Cu(II) and H^+ ions onto the active sites of PAANA [34, 35].

The possible Cu(II) ion adsorption mechanisms by the PAANA sample are illustrated in Scheme 2. The PAANA matrix is a 3D network of PAA chains with different functional groups (e.g., $-\text{COOH}$ and $-\text{COO}^-$). At moderate $\text{pH} = 5$, where $\text{pH} > \text{pK}_a$ of PAA (4.3), the $-\text{COOH}$ groups dissociate and deprotonate as $-\text{COO}^-$ [16]. Cu(II) ions penetrate the PAANA network and are attracted by the negatively charged $-\text{COO}^-$ through electrostatic interactions. Ion exchange may also occur between Na^+ cations in the matrix and Cu(II) ions [22]. After being attracted by the negatively charged functional groups, the Cu(II) ions start to coordinate $-\text{COO}^-$ groups to form a stable structure through a complexation interaction, as evidenced by the FTIR results in Fig. 1b. Since the PAANA sample had maximum adsorption efficiency for Cu(II) ions at $\text{pH} = 5$, this pH was selected as the parameter for further adsorption and recovery experiments.

Adsorption kinetics

The effects of contact time on the adsorption capacities of Cu(II) ions by the PAANA samples at initial concentrations of $25\text{--}100 \text{ mg dm}^{-3}$ are shown in Fig. 4a. At all initial Cu(II) ion concentrations ($25\text{--}100 \text{ mg dm}^{-3}$), adsorption occurred rapidly within the first 6 h of exposure, reaching equilibrium within 24 h, indicating the rapid adsorption kinetics of the PAANA sample. With the increase of Cu(II) ion initial concentration from 25 to 100 mg dm^{-3} , the adsorption capacity (q_e) of the PAANA sample increased (from 83.98 to 226.83 mg g^{-1}) significantly at equilibrium, which may be attributed to a much stronger driving force

Scheme 2 Schematic diagram of the PAANa sample structure before and after Cu(II) adsorption



for the mass transfer and subsequent surface adsorption onto the PAANa matrix at higher concentrations [36, 37].

The adsorption capacity of Cu(II) ions onto the PAANa sample was investigated by two empirical power law models: pseudo-first- and second-order kinetic models. Empirical first- and second-order kinetic models are expressed by Eq. 4, for reaction exponents $n = 1$ and 2, respectively [38]:

$$\frac{dq_t}{dt} = k_n(q_e - q_t)^n, \quad (4)$$

where q_t (mg g^{-1}) and q_e (mg g^{-1}) represent adsorption capacity at contact time t and at equilibrium, respectively. k_1 and k_2 are the first- and second-order kinetic rate constants, respectively. Integrating Eq. 4 with the boundary conditions $t = 0$, $q_t = 0$, and $t = t$, $q_t = q_t$ to the linear form gives Eqs. 5 and 6, respectively:

$$\log(q_e - q_t) = \log q_e - \frac{k_1}{2.303} t \quad (5)$$

$$\frac{t}{q_t} = \frac{1}{k_2 q_e^2} + \frac{t}{q_e}. \quad (6)$$

The rate constants k_1 and k_2 can be determined from the slope of the linear plots of $\log(q_e - q_t)$ versus t and the

intercept of the linear plot between t/q_t versus t , respectively.

We used both pseudo-first-order and pseudo-second-order kinetic models to fit the experimental data (Fig. 4b, c), and the regression coefficients (R^2) data (Table 1) indicate that the experimental kinetic data for the adsorption of Cu(II) ions onto the PAANa sample fit much better to a pseudo-second-order model ($R^2 > 0.999$) than to a pseudo-first-order model ($R^2 > 0.779$). Furthermore, the pseudo-second-order model estimates q_e values (Table 1) in good agreement with the experimental values q_e (exp). Thus, the empirical second-order model is suitable for the description of the adsorption kinetics of Cu(II) ions onto the PAANa sample. These results are consistent with those in the literature [16, 18, 39]. In most cases in the literature, the pseudo-first-order kinetic equation only fitted well for the initial stage of contact time (e.g., <30 min) of an adsorption process and the estimated q_e values derived from this equation were not in good agreement with the experimental q_e values [18]. The k_2 data (Table 1) indicate that at low Cu(II) concentration (25 mg dm^{-3}) the initial adsorption rate for the PAANa sample is much higher and the adsorption can reach equilibrium more rapidly than in the solution with higher Cu(II) concentration (100 mg dm^{-3}).

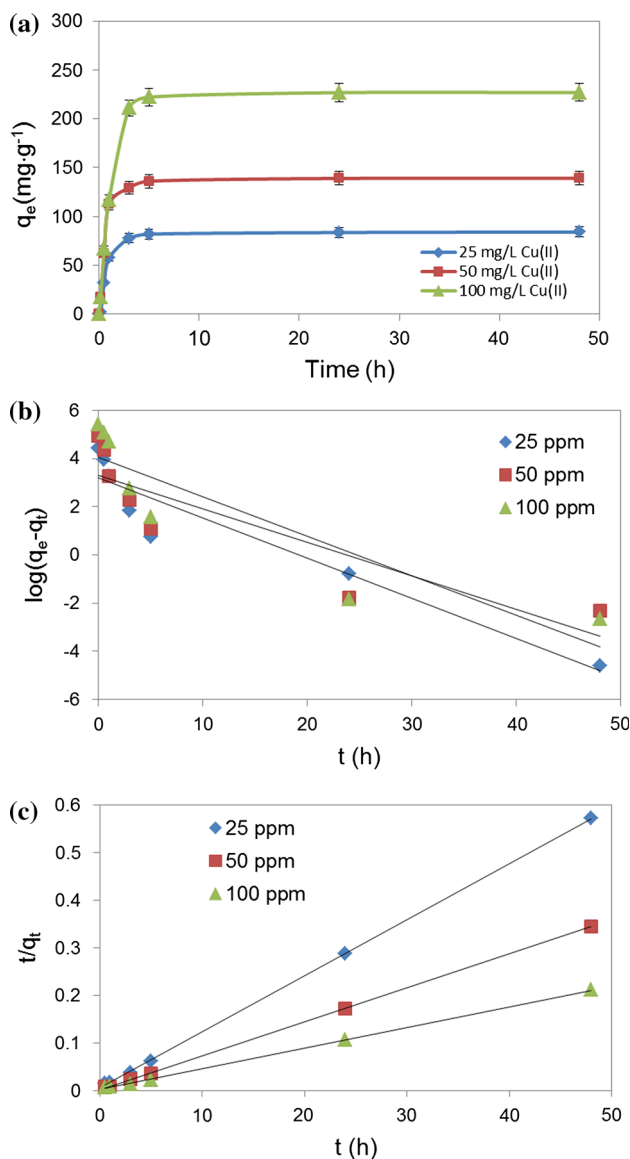


Fig. 4 **a** Adsorption kinetics of PAANa sample (prepared by 0.45 g cm⁻³ NaOH solution) at different initial concentrations of Cu(II) ions (25–100 mg dm⁻³) (contact time: 24 h, pH = 5), **b** pseudo-first-order kinetic plot and **c** pseudo-second-order kinetic plot

Adsorption isotherms

The influence of equilibrium concentrations C_e on adsorption capacities of Cu(II) ions onto PAANa sample is shown in Fig. 5a. The Cu(II) ions adsorbed onto the adsorbent increase with the increasing Cu(II) ion concentration and reach a plateau after the equilibrium concentrations C_e reach ~ 100 mg dm⁻³, which is due to the greater driving force of the concentration gradient at the solid–liquid interface at a higher Cu(II) ion concentration [16].

To predict the equilibrium parameters of adsorption isotherms and to describe adsorption properties, Langmuir and Freundlich isotherms are commonly used for the molecular adsorption at interfaces [38]. A monolayer coverage of the adsorbates onto the energetically equivalent active sites of a structurally homogeneous adsorbent is presumed by the Langmuir model, which is expressed as Eq. 7 [40]

$$\frac{C_{eq}}{q_e} = \frac{1}{q_{max}b} + \frac{C_{eq}}{q_{max}}, \tag{7}$$

where q_e and C_{eq} are the adsorption capacity (mg g⁻¹) and Cu(II) ion concentration (mg dm⁻³) at equilibrium, respectively. b and q_{max} are the Langmuir constant (dm³ mg⁻¹) and maximum adsorption capacity (mg g⁻¹) determined by the intercept and slope of the linear plot of C_{eq}/q_e versus C_{eq} .

The Freundlich isotherm used to describe adsorption onto a heterogeneous system with uniform energy without restriction to the formation of a monolayer can be expressed as [41]

$$\log q_e = \log K_f + \frac{1}{n} \log C_{eq}, \tag{8}$$

where K_f and $1/n$ are the Freundlich adsorption constant (dm³ mg⁻¹) and adsorption intensity (dimensionless), respectively. The parameters may be, respectively, calculated from the intercept and slope of the plot of $\log q_e$ versus $\log C_{eq}$.

Table 1 Pseudo-first-order and pseudo-second-order kinetic parameters of Cu(II) adsorption onto PAANa (prepared by 0.45 g cm⁻³ NaOH solution) sample

| Sample | Cu(II) (mg dm ⁻³) | Pseudo-first-order model | | | | Pseudo-second-order model | | |
|--------|-------------------------------|-----------------------------------|--------------------------|--------------------------------|-------|---|-----------------------------------|-------|
| | | q_e (exp) (mg g ⁻¹) | k_1 (h ⁻¹) | q_e (cal) mg g ⁻¹ | R^2 | k_2 (g mg ⁻¹ h ⁻¹) | q_e (cal) (mg g ⁻¹) | R^2 |
| PAANa | 25 | 83.89 | 0.3851 | 24.82 | 0.907 | 0.0268 | 84.75 | 0.999 |
| | 50 | 139.05 | 0.3201 | 27.46 | 0.779 | 0.0229 | 140.85 | 0.999 |
| | 100 | 226.83 | 0.3786 | 57.98 | 0.811 | 0.0066 | 232.56 | 0.999 |

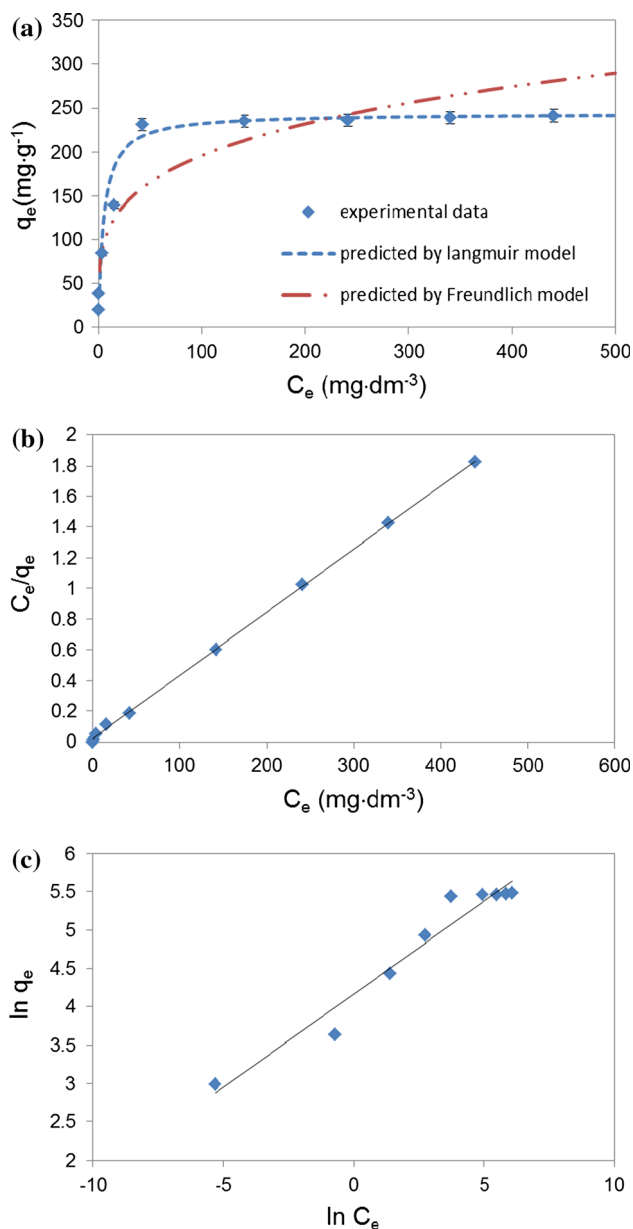


Fig. 5 **a** Adsorption isotherms of PAANa sample (prepared by 0.45 g cm⁻³ NaOH solution, contact time: 24 h, pH = 5), **b** Langmuir model adsorption isotherm plot, and **c** Freundlich model adsorption isotherm plot

The experimental data were fitted using the Langmuir and Freundlich modes (Fig. 5 b, c), and the regression coefficients (R^2) data in Table 2 indicate that the Langmuir model ($R^2 = 0.999$) described the Cu(II) adsorption

Table 2 Langmuir and Freundlich isotherm parameters of PAANa sample (prepared by 0.45 g cm⁻³ NaOH solution)

| Sample | Langmuir model | | | Freundlich model | | |
|--------|---|----------------------------------|-------|---|-------|-------|
| | b (dm ³ mg ⁻¹) | q_{\max} (mg g ⁻¹) | R^2 | K_f (dm ³ mg ⁻¹) | n | R^2 |
| PAANa | 0.199 | 243.91 | | 64.05 | 4.117 | 0.951 |

process onto the PAANa sample much better than the Freundlich model ($R^2 = 0.951$). Thus, a Langmuir adsorption isotherm can be used for the best description of the observed adsorption equilibrium behavior of Cu(II) ions onto PAANa adsorbent and the adsorption may be assumed to be a monolayer coverage of adsorbate at homogeneous binding sites on the adsorbents [21, 34, 42].

The PAANa sample has the maximum adsorption capacity of 243.91 mg g⁻¹ predicted by the Langmuir model (Table 2), which is higher than that of other conventional low-cost materials and polymers (Table 3). The superior adsorption efficiency for Cu(II) ions may be ascribed to the presence of $-\text{COO}^-$ and $-\text{COOH}$ groups in the PAANa matrix which has strong propensity for the complexation of Cu(II) ions [16, 18, 22, 29].

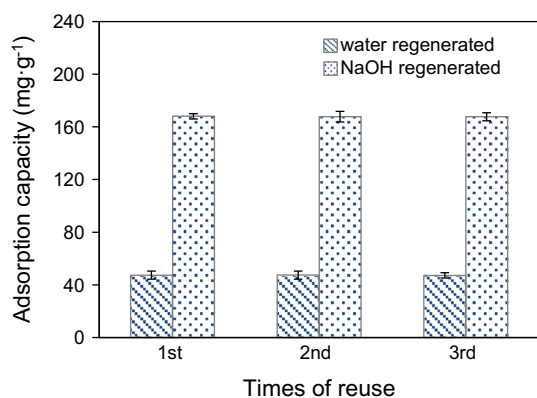
Desorption and regeneration

The desorption of Cu (II) ions from the PAANa sample was studied using 0.01 M nitric acid solution, and the recovery of adsorbed copper was found to be 98.92 %. This confirms the good evaluation of PAANa material for copper adsorption and recovery. The remaining copper on the adsorbent may be due to the high affinity of Cu(II) toward functional groups (e.g., $-\text{COO}^-$) deep within the PAANa matrix, which could lead to a very slow recovery process.

Desorption of Cu(II) can also be used to regenerate the PAANa composite, which can be used again to adsorb metal ions. To investigate the recyclability of the PAANa sample, consecutive adsorption–desorption processes were performed three times with 0.01 M nitric acid solution as the desorption solution and Milli-Q water or 3.5×10^{-4} M sodium hydroxide solution as the regeneration solution. Figure 6 shows the adsorption capacities for Cu(II) of the PAANa sample after three successive adsorption–desorption cycles. The adsorption capacity after first cycle decreases to 47.38 and 168.15 mg·g⁻¹ regenerated by Milli-Q water and sodium hydroxide solution, respectively, which are 19.43 and 68.93 % of the pristine PAANa sample adsorption capacity. No further decrease of the Cu(II) adsorption capacity was observed by both regeneration solutions after 2 or 3 regenerations. 0.01 M nitric acid was used as the desorption solution (acid-treated process) and the regenerated sample was dried in an oven for 24 h (heating process), which could have caused the decrease of the adsorption capacity of the PAANa sample after regeneration [16]. Compared with Milli-Q water, a very

Table 3 Comparison of maximum adsorption capacities for Cu(II) ions of different adsorbents

| Sample | q_{\max} (mg g ⁻¹) | References |
|---|----------------------------------|------------|
| Activated carbon | 17.83 | [43] |
| Graphene oxide/zeolite | 28.58 | [34] |
| Chitosan | 85.21 | [44] |
| Chitosan-g-poly(acrylic acid)/attapulgitite composites | 170.65–262.25 | [16] |
| Starch-g-PAA/sodium humate hydrogels | 167.01–179.71 | [18] |
| Poly(polyethylene glycol diacrylate) or poly(methacrylic acid) polymers | 22.86–78.74 | [45] |
| Graphene oxide/chitosan | 70.00 | [46] |
| Alginate-based hydrogel | 184.85 | [22] |
| Sodium polyacrylate bead | 58.82 | [39] |
| PAANa | 243.91 | This work |

**Fig. 6** Adsorption capacity of PAANa sample (prepared by 0.45 g cm⁻³ NaOH solution, contact time: 24 h, pH = 5) after 3 regeneration processes by Milli-Q water or 3.5 × 10⁻⁴ M NaOH solution

low concentration of NaOH is a superior regeneration agent which restores ~69 % of the adsorption capacity of the PAANa sample. This is because some of the –COOH groups in the PAANa matrix after regeneration by acid can be converted into –COO⁻ Na⁺ groups by the NaOH solution, which has a strong affinity for ion exchange and complexation with Cu(II) ions in aqueous solution [18]. The average desorption efficiency of the PAANa sample was relatively high (~69 %) and stable after three consecutive adsorption–desorption processes, indicating that this composite can be potentially regenerated and reused as a low-cost, environmentally friendly adsorbent.

Conclusions

Superabsorbent polymers (SAP) based on poly(acrylic acid) (PAA) were successfully synthesized through a novel one-step cost-effective method. The PAANa sample prepared by 0.45 g cm⁻³ NaOH solution showed significantly higher adsorption capacity than other PAA-based samples at moderate pH values, due to the presence of functional

groups (–COOH and –COO⁻) in the polymer matrix and a higher water absorption capacity (WAC). The adsorption capacity for Cu(II) was influenced by the pH of the solution, and maximum adsorption was observed at pH = 5. The Cu(II) adsorption reached equilibrium within 6 h, resulting in the maximum adsorption capacity of 243.91 mg g⁻¹ by the PAANa sample. 98.92 % of the adsorbed copper was recovered in 0.01 M of nitric acid from the Cu(II)-loaded PAANa sample. The PAANa sample retained ~69 % of its original adsorption capacity after three consecutive adsorption–desorption cycles, indicating that the PAANa composite could be recycled and reused as an effective adsorbent for Cu(II) recovery.

Acknowledgements Y Tang is grateful for the support of the Australian Research Council (ARC) with a Discovery Early Career Researcher Award (DECRA) Grant (DE120102784) for the research work.

Conflict of interest The authors declare that they have no conflict of interest.

References

- Anirudhan TS, Rijith S (2009) Glutaraldehyde cross-linked epoxyaminated chitosan as an adsorbent for the removal and recovery of copper(II) from aqueous media. *Colloids Surf A* 351:52–59
- Chan A, Salsali H, McBean E (2014) Heavy metal removal (copper and zinc) in secondary effluent from wastewater treatment plants by microalgae. *ACS Sustain Chem Eng* 2:130–137
- Gollavelli G, Chang CC, Ling YC (2013) Facile synthesis of smart magnetic graphene for safe drinking water: heavy metal removal and disinfection control. *ACS Sustain Chem Eng* 1:462–472
- Chiron N, Guilet R, Deydier E (2003) Adsorption of Cu(II) and Pb(II) onto a grafted silica: isotherms and kinetic models. *Water Res* 37:3079–3086
- Chang JH, Ellis AV, Tung CH, Huang WC (2010) Copper cation transport and scaling of ionic exchange membranes using electro-dialysis under electroconvection conditions. *J Membr Sci* 361:56–62
- Unuabonah EI, Günter C, Weber J, Lubahn S, Taubert A (2013) Hybrid clay: a new highly efficient adsorbent for water treatment. *ACS Sustain Chem Eng* 1:966–973

7. Ayoub A, Venditti RA, Pawlak JJ, Salam A, Hubbe MA (2013) Novel hemicellulose-chitosan biosorbent for water desalination and heavy metal removal. *ACS Sustain Chem Eng* 1:1102–1109
8. Liu P, Jiang L, Zhu L, Wang A (2014) Attapulgite/poly(acrylic acid) nanocomposite (ATP/PAA) hydrogels with multifunctionalized attapulgite (org-ATP) nanorods as unique cross-linker: preparation optimization and selective adsorption of Pb(II) Ion. *ACS Sustain Chem Eng* 2:643–651
9. Hashim MA, Mukhopadhyay S, Sahu JN, Sengupta B (2011) Remediation technologies for heavy metal contaminated groundwater. *J Environ Manag* 92:2355–2388
10. Gong JP, Katsuyama Y, Kurokawa T, Osada Y (2003) Double-network hydrogels with extremely high mechanical strength. *Adv Mater* 15:1155–1158
11. Zohuriaan-Mehr MJ, Kabiri K (2008) Superabsorbent polymer materials: a review. *Iran Polym J* 17:451–477
12. Wang Q, Mynar JL, Yoshida M, Lee E, Lee M, Okuro K, Kinbara K, Aida T (2010) High-water-content mouldable hydrogels by mixing clay and a dendritic molecular binder. *Nature* 463:339–343
13. Zheng Y, Wang A (2010) Enhanced adsorption of ammonium using hydrogel composites based on chitosan and halloysite. *J Macromol Sci Pure Appl Chem* 47:33–38
14. Haraguchi K, Takehisa T (2002) Nanocomposite hydrogels: a unique organic-inorganic network structure with extraordinary mechanical, optical, and swelling/De-swelling properties. *Adv Mater* 14:1120–1124
15. Estrada AC, Daniel-Da-Silva AL, Trindade T (2013) Photothermally enhanced drug release by κ -carrageenan hydrogels reinforced with multi-walled carbon nanotubes. *RSC Adv* 3:10828–10836
16. Wang X, Zheng Y, Wang A (2009) Fast removal of copper ions from aqueous solution by chitosan-g-poly(acrylic acid)/attapulgite composites. *J Hazard Mater* 168:970–977
17. Xu X, Bai B, Ding C, Wang H, Suo Y (2015) Synthesis and properties of an ecofriendly superabsorbent composite by grafting the poly(acrylic acid) onto the surface of dopamine-coated sea buckthorn branches. *Ind Eng Chem Res* 54:3268–3278
18. Zheng Y, Hua S, Wang A (2010) Adsorption behavior of Cu^{2+} from aqueous solutions onto starch-g-poly(acrylic acid)/sodium humate hydrogels. *Desalination* 263:170–175
19. Wu N, Li Z (2013) Synthesis and characterization of poly(HEA/MALA) hydrogel and its application in removal of heavy metal ions from water. *Chem Eng J* 215–216:894–902
20. Laftah WA, Hashim S (2012) Synthesis, optimization, characterization and agricultural field evaluation of polymer hydrogel composites based on poly acrylic acid and micro-fiber of oil palm empty fruit bunch. *Int J Plast Technol* 16:166–181
21. Yu Y, Addai-Mensah J, Losic D (2012) Functionalized diatom silica microparticles for removal of mercury ions. *Sci Technol Adv Mater* 13(1):015008
22. Wang W, Kang Y, Wang A (2013) One-step fabrication in aqueous solution of a granular alginate-based hydrogel for fast and efficient removal of heavy metal ions. *J Polym Res* 20:101–110
23. Zhang J, Wang Q, Wang A (2007) Synthesis and characterization of chitosan-g-poly(acrylic acid)/attapulgite superabsorbent composites. *Carbohydr Polym* 68:367–374
24. Wang J, Wang W, Wang A (2010) Synthesis, characterization and swelling behaviors of hydroxyethyl cellulose-g-poly(acrylic acid)/attapulgite superabsorbent composite. *Polym Eng Sci* 50:1019–1027
25. Ibrahim M, Nada A, Kamal DE (2005) Density functional theory and FTIR spectroscopic study of carboxyl group. *Indian J Pure Appl Phys* 43:911–917
26. Larsen OFA, Woutersen S (2004) Vibrational relaxation of the H_2O bending mode in liquid water. *J Chem Phys* 121:12143–12145
27. Finocchio E, Macis E, Raiteri R, Busca G (2007) Adsorption of trimethoxysilane and of 3-mercaptopropyltrimethoxysilane on silica and on silicon wafers from vapor phase: an IR study. *Langmuir* 23:2505–2509
28. Ismi I, Rifi EH, Lebkiri A, Oudda H (2015) Spectral characterization of pana under two polymeric forms and their complex PA-Cu. *J Mater Environ Sci* 6:343–348
29. Çavuş S, Gürdağ GL (2009) Noncompetitive removal of heavy metal ions from aqueous solutions by poly[2-(acrylamido)-2-methyl-1-propanesulfonic acid-co-itaconic acid] hydrogel. *Ind Eng Chem Res* 48:2652–2658
30. Pourjavadi A, Soleyman R, Barajee GR (2008) Novel nanoporous superabsorbent hydrogel based on poly(acrylic acid) grafted onto salep: synthesis and swelling behavior. *Starch* 60:467–475
31. Sugahara Y, Ohta T (2001) Synthesis of starch-graft-polyacrylonitrile hydrolyzate and its characterization. *J Appl Polym Sci* 82:1437–1443
32. Lee CI, Yang WF, Chio CS (2006) Utilization of water clarifier sludge for copper removal in a liquid fluidized-bed reactor. *J Hazard Mater* 129:58–63
33. Zhang S, Shu X, Zhou Y, Huang L, Hua D (2014) Highly efficient removal of uranium (VI) from aqueous solutions using poly(acrylic acid)-functionalized microspheres. *Chem Eng J* 253:55–62
34. Yu Y, Shapter JG, Popelka-Filcoff R, Bennett JW, Ellis AV (2014) Copper removal using bio-inspired polydopamine coated natural zeolites. *J Hazard Mater* 273:174–182
35. Lin J, Zhan Y, Zhu Z (2011) Adsorption characteristics of copper(II) ions from aqueous solution onto humic acid-immobilized surfactant-modified zeolite. *Colloids Surf A* 384:9–16
36. Yu Y, Murthy BN, Shapter JG, Constantopoulos KT, Voelcker NH, Ellis AV (2013) Benzene carboxylic acid derivatized graphene oxide nanosheets on natural zeolites as effective adsorbents for cationic dye removal. *J Hazard Mater* 260:330–338
37. Al-Ghouthi MA, Khraisheh MAM, Ahmad MNM, Allen S (2009) Adsorption behaviour of methylene blue onto Jordanian diatomite: a kinetic study. *J Hazard Mater* 165:589–598
38. Ho YS (2004) Selection of optimum sorption isotherm. *Carbon* 42:2115–2116
39. Ismi I, Elaidi H, Rifi E, Labkiri A, Skalli A (2014) Kinetics and isotherms studies on Cu^{2+} adsorption onto PANa bead form from aqueous solutions. *Inter J Sci Eng Res* 5:701–706
40. Kraus A, Jainae K, Unob F, Sukpirom N (2009) Synthesis of MPTS-modified cobalt ferrite nanoparticles and their adsorption properties in relation to Au(III). *J Colloid Interface Sci* 338:359–365
41. Freundlich HMF (1906) Over the adsorption in solution. *J Phys Chem* 57:385–470
42. Baba Y, Ohe K, Kawasaki Y, Kolev SD (2006) Adsorption of mercury(II) from hydrochloric acid solutions on glycidyl-methacrylate-divinylbenzene microspheres containing amino groups. *React Funct Polym* 66:1158–1164
43. Alslaihi TM, Abustan I, Ahmad MA, Foul AA (2013) Kinetics and equilibrium adsorption of iron(II), lead(II), and copper(II) onto activated carbon prepared from olive stone waste. *Desalin Water Treat* 52:7887–7897
44. Kołodnyńska D (2011) Chitosan as an effective low-cost sorbent of heavy metal complexes with the polyaspartic acid. *Chem Eng J* 173:520–529
45. Wang J, Liu F, Wei J (2011) Enhanced adsorption properties of interpenetrating polymer network hydrogels for heavy metal ion removal. *Polym Bull* 67:1709–1720
46. Chen Y, Chen L, Bai H, Li L (2013) Graphene oxide-chitosan composite hydrogels as broad-spectrum adsorbents for water purification. *J Mater Chem A* 1:1992–2001